

pubs.acs.org/ac Article

Second Harmonic Generation Interrogation of the Endonuclease APE1 Binding Interaction with G-Quadruplex DNA

Aaron M. Fleming, Renee Tran, Carla A. Omaga, Shereen A. Howpay Manage, Cynthia J. Burrows,* and John C. Conboy*



Cite This: Anal. Chem. 2022, 94, 15027–15032



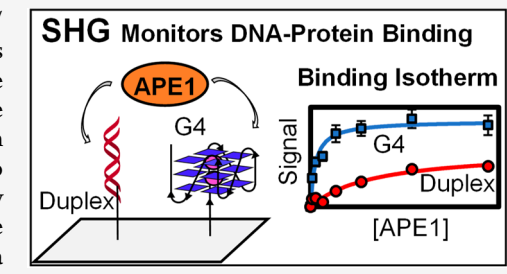
ACCESS I

III Metrics & More

Article Recommendations

SI Supporting Information

ABSTRACT: The binding interaction between the DNA repair enzyme apurinic/apyrimidinic endonuclease-1 (APE1) with promoter G-quadruplex (G4) folds bearing an abasic site (AP) can serve as a gene regulatory switch during oxidative stress. Prior fluorescence-based analysis in solution suggested APE1 binds the VEGF promoter G4 but whether this interaction was specific or not remained an open question. Second harmonic generation (SHG) was used in this work to measure the noncanonical DNA—protein binding interaction in a label-free assay with high sensitivity to demonstrate the interaction is ordered and specific. The binding of APE1 to the VEGF promoter G4 with AP sites modeled by a tetrahydrofuran analogue produced dissociation constants of \sim 100 nM that



differed from duplex and single-stranded DNA control studies. The SHG measurements confirmed APE1 binds the VEGF G4 folds in a specific manner resolving a remaining question regarding how this endonuclease with gene regulatory features engages G4 folds. The studies demonstrate the power of SHG to interrogate noncanonical DNA—protein interactions providing a foundational example for the use of this analytical method in future biochemical analyses.

■ INTRODUCTION

Interactions between proteins and DNA facilitate many critical biological processes, including DNA repair, gene regulation, and cellular replication. Methylation of the cytosine base alters DNA-protein interactions for fine-tuning cellular processes termed epigenetic regulation. Recent cellular studies have found during reactive oxygen species (ROS)-induced oxidative stress, another set of epigenetic-like DNA modifications is functional in the form of oxidation of the guanine (G) base to 8-oxo-7,8-dihydroguanine (OG).^{2,3} One mode in this regulatory pathway functions in G-rich gene promoters, in which facile formation of OG occurs and initiates DNA repair for release of OG by OG glycosylase 1 (OGG1) to yield an abasic site (AP) in duplex DNA. The AP destabilizes the duplex, and through the coordinated binding by apurinic/apyrimidinic endonuclease-1 (APE1), the duplex is remodeled to a Gquadruplex (G4) structure in certain G-rich sequences (Figure 1A).^{2,4} The AP-containing G4 interaction with APE1 is proposed to serve as a hub for regulatory factor binding to induce mRNA synthesis during oxidative stress. This DNAprotein binding is the critical interaction for the epigenetic-like

Sequences of DNA with four or more runs of three G nucleotides in each run that are in proximity have the potential to adopt G4 folds. G-Quadruplexes are held together by G:G Hoogsteen base pairs forming G-tetrads that stack and coordinate to K^+ ions in cells (Figure 1B). Based on the sequence, G4s can have G nucleotides in the loop or core

position of the structure. The vascular endothelial growth factor (VEGF) gene was demonstrated to be activated by G oxidation in the promoter followed by DNA repair-induced remodeling of the duplex to a G4 fold, in which APE1 bound the noncanonical structure for gene induction.² The binding interaction between the VEGF gene promoter G4 and APE1 has been interrogated by fluorescence-based experiments in solution.4 The studies found APE1 binds the AP-containing G4 with nanomolar dissociation constants (K_d) with dependency on the ionic strength and the proposed protein binding sites include the nuclease domain as well as the intrinsically disordered N-terminal domain. Equally interesting was the finding that APE1 bound the G4 without an AP with the lowest K_d value measured, which occurred via the N-terminal domain. A challenge with measuring DNA-protein binding via fluorescence anisotropy is the inability to rule out nonspecific interactions between the positively charged protein and the negatively charged DNA during the binding experiment. This unknown remained unresolved in our prior studies, and the present work showcases an analytical approach to interrogate

Received: July 8, 2022 Accepted: October 10, 2022 Published: October 21, 2022





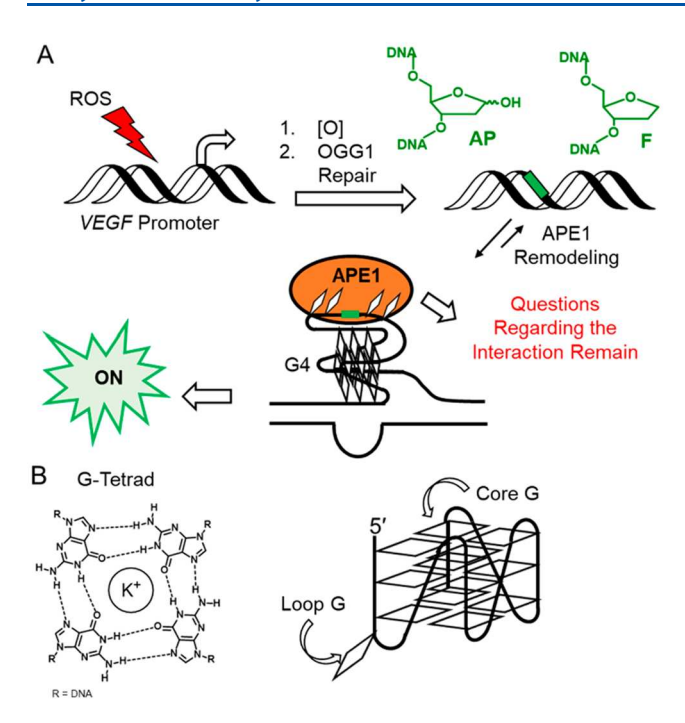


Figure 1. (A) APE1 binding to a promoter G4 functions as a regulatory hub for gene induction during oxidative stress. (B) G-Quadruplexes are comprised of G-tetrads that adopt G4 folds with G nucleotides in either loop or core positions.

noncanonical DNA-protein interactions without the challenges associated with fluorescence experiments.⁴

To address this uncertainty, second harmonic generation (SHG) was utilized to study the binding interaction between APE1 and the VEGF G4 folds with and without an AP present. SHG enables high sensitivity and label-free detection of the VEGF G4-APE1 interaction without the need for an exogenous reporter such as a fluorophore or protein conjugate. The surface specificity, high sensitivity, and insensitivity to randomly ordered nonspecific adsorption make SHG a viable label-free alternative to other assays and one that is capable of providing limits of detection (LODs) similar to those seen in the fluorescence-based assays. Assays capable of overcoming the limitations associated with labeling proteins for the investigation of biomolecular interactions have a clear advantage, with SHG being the most recent addition. Noteworthy examples include studies utilizing SHG to measure HIV-1 GAG association with lipid membranes, melittin insertion into a lipid bilayer, a comparison of avidin, streptavidin, neutrAvidin, and antibiotin antibody binding to biotinylated lipid bilayers, ¹⁰ following DNA binding and cleavage by an endonuclease, ¹¹ and SHG correlation spectroscopy methods enable retrieving biological binding kinetics. 12 Herein, SHG was employed to study the APE1-VEGF G4 binding interaction.

■ EXPERIMENTAL SECTION

Preparation of DNA Strands and Protein. All DNA strands were synthesized and deprotected by the DNA/Peptide core facility of the University of Utah following standard protocols. The site-specific introduction of the AP analogue was achieved using the commercially available tetrahydrofuran (F) phosphoramidite. Authentic APs are chemically unstable and degrade to strand breaks, whereas F

is stable for study and equally well recognized by APE1. ¹³ The sequences studied were synthesized with a 3'-sulfhydryl connected to a polyT₁₀ through a hexyl linker to facilitate surface immobilization as described below. As previously described, the synthesized strands were purified, stored, and prepared for analysis. ⁴ Human wild-type APE1 was expressed from the pET28HIS-hAPE1 plasmid deposited in the Addgene repository (#70757) following the literature protocol for this protein overexpression plasmid. ¹⁴ Analysis of the G4 folds by circular dichroism (CD) spectroscopy and APE1 endonuclease assays were conducted following literature methods. ⁴ Complete experimental details regarding these experiments are provided in the Supporting Information file.

SHG Measurements. All DNA strands used in this study had a 3'-sulfhydryl connected to a polyT₁₀ through a hexyl linker that enabled the DNA to be attached to the surface via a thiol reaction with maleimide. The VEGF, VEGF-F14, VEGF-F12, poly-T₂₀, or poly-TF (poly-T₂₀ with a centrally located F residue) sequences were immobilized on the surface of a fused silica prism, which was cleaned using a 70:30 solution of sulfuric acid:hydrogen peroxide before use. Caution: This solution reacts violently with organic solvents. Extreme caution must be exercised when handling this solution. The prism was coated with a 2% solution of (3-aminopropyl)triethoxysilane (APTES) in acetone, followed by a rinse with excess acetone. A 2 mg/mL solution of sulfosuccinimidyl 4-(Nmaleimidomethyl)cyclohexane-1-carboxylate (sulfo-SMCC) in PBS was incubated with the APTES-coated surface for 1 h, followed by a rinse with excess buffer, before mounting in a custom Teflon flow cell. The oligonucleotide to be immobilized was initially incubated at room temperature for 1 h and then incubated overnight at 4 °C.

APE1 Binding Studies. Adsorption isotherms of APE1 binding to VEGF, VEGF-F14, and VEGF-F12 in G4 or duplex contexts in addition to adsorption isotherms of APE1 binding to the single-stranded poly-T20 or poly-TF strands were collected using a counterpropagating SHG setup, described previously. The immobilized DNA surface was passivated by washing with 1 mg/mL BSA until the SHG intensity stopped increasing, followed by a rinse with PBS. To form DNA duplexes, the VEGF complementary strand was injected in increasing concentrations ranging from 10 nM to 1 μ M over the immobilized DNA until saturation was achieved as determined by a constant SHG intensity. The analysis was conducted in 50 mM PBS, 50 mM KCl, and 2 mM EDTA at pH 7.4. Concentrations of APE1 ranging from 10 nM to 1 μ M were injected into the flow cell that contained either ssDNA or duplex DNA. A single concentration was injected into the flow cell until steady-state equilibrium was attained, which was taken as a constant SHG intensity. The resulting binding isotherms were fit using the Langmuir isotherm model. All data were normalized for day-to-day laser fluctuations and alignment of the collection optics by dividing the SHG intensity at each concentration by the SHG intensity of a 10 mM KOH solution measured at the end of each experiment. Due to the nonlinear nature of SHG, the measured intensity (I_{SHG}) is proportional to the square of the number of proteins binding to the DNA at the surface (eq 1).

$$I_{SHG} = \Gamma_{APE1}^2 \tag{1}$$

To convert the SHG intensity to a relative percent capture efficiency, the square root of the SHG intensity was taken,

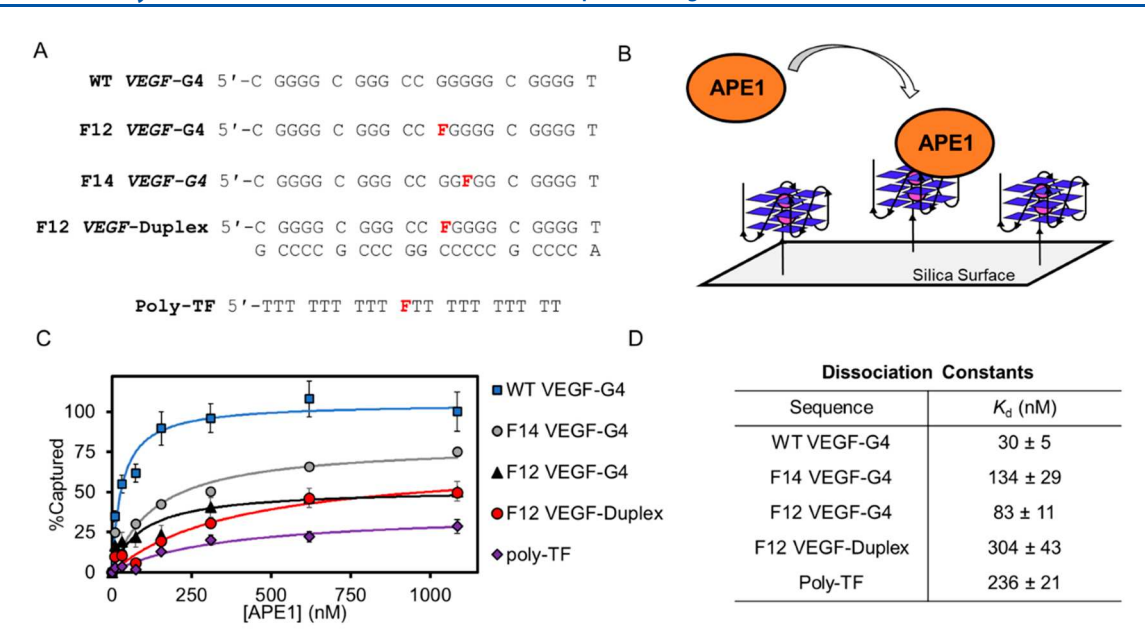


Figure 2. Binding between APE1 and the VEGF sequences monitored by SHG. (A) DNA sequences studied had a 3'-sulfhydryl attached to T_{10} via a hexyl linker installed by standard synthetic methods (not shown). (B) Illustration of the SHG experimental setup. (C) SHG-derived isotherms were used to compute the (D) K_d values for the interaction. Error bars represent the average of three replicate measurements, with the computed dissociation constants obtained from a Langmuir binding model listed in the panel D table.

divided by the maximum intensity at surface saturation, and multiplied by 100.

APE1 Desorption and Release. After saturating the immobilized DNA with APE1 as described above, the flow cell was rinsed with excess PBS, and the resulting SHG intensity was measured over time to determine the dissociation constant of the APE1–DNA complex. To restore the cleavage activity of APE1, excess PBS–Mg²⁺ was injected over the bound APE1–DNA complex. The decay in SHG intensity was measured and used to obtain the rate of APE1 release.

RESULTS AND DISCUSSION

For the wild-type APE1 binding studies interrogated by SHG, the analysis was conducted without Mg²⁺ present and excess EDTA (2 mM) to avoid cleavage of the strands at the AP (model with a tetrahydrofuran analogue F). Our prior studies demonstrated this strategy diminished the endonuclease activity of APE1 to a level below detectable limits based on gel electrophoresis analysis.⁴ The DNA sequences studied are provided in Figure 2A, and the wild-type APE1 was generated by standard recombinant methods following a literature protocol (Figure S1).4 Before the commencement of the binding studies, the folding of the sequences to G4s was verified by CD spectroscopy (Figure S2). The VEGF sequences were annealed to adopt G4 folds or adopt a duplex with the addition of the complementary strand. The VEGF G4s are unimolecular, in which their folding is triggered by K+ ions that are present in large excess (50 mM); 15 when these sequences are surface bound via a poly-T₁₀ linker at low surface density, they will likely maintain unimolecular folding. Prior studies found the duplex DNA structure is maintained under the conditions of the present study, 11 which also suggests binding to the surface will have negligible impact on the G4 folds. The binding of APE1 to the surface-bound target DNA strands produced binding isotherms that were fit to a Langmuir isotherm to determine the K_d values for the interaction (Figure 2B-D) using eq 2:

$$\frac{I_{SHG}^{1/2}}{I_{max}^{1/2}} = \frac{[APE1]}{K_d + [APE1]}$$
 (2)

where I_{SHG} is the SHG intensity, I_{max} is the SHG intensity at binding saturation, K_d is the dissociation constant, and [APE1] is the solution concentration of APE1. A titration of APE1 to be bound with surface-immobilized DNA was conducted, and the signals were monitored at each protein concentration until saturation was achieved (Figure 2B,C). The ability to measure and quantify APE1 binding in a label-free manner is due to resonant enhancement of the SHG signal. Specifically, the UV absorption due to the π to π^* electronic transitions of the aromatic amino acids in the APE1 protein are commensurate with the second harmonic emission. Second Triplicate binding isotherms were obtained using the normalization procedure described previously.

First, a single-stranded DNA standard comprised of a T₂₀ strand with a centrally located F residue (poly-TF) was found to have a K_d of 236 \pm 21 nM for the DNA-protein interaction (Figure 2C,D). Interrogation of a duplex DNA control strand formed from the VEGF potential G4 sequence with F at position 12 produced a K_d value of 304 \pm 43 nM (Figure 2B,C). In the absence of the complementary strand, the folded VEGF G4 with an F in a core position (position 14) was bound by APE1 with a K_d value of 134 \pm 29 nM, while the G4 with F in a loop position (position 12) produced a K_d value of 83 \pm 11 nM (Figure 2C,D). The final sequence studied in the VEGF G4 sequence series was the native G4 fold with all G nucleotides, for which the APE1-G4 interaction produced a K_d value of 30 \pm 5 nM, which was the tightest binding constant measured (Figure 2B,C). The SHG analysis found nanomolar K_d values for the APE1 binding the DNA with dependency on the structure and sequence of the DNA substrate.

A few control experiments were conducted to verify that the binding interactions occur through native domains in APE1 and the binding stochiometry was 1:1. We used recombinant APE1 purified with a C-terminal hexahistidine tag that was not

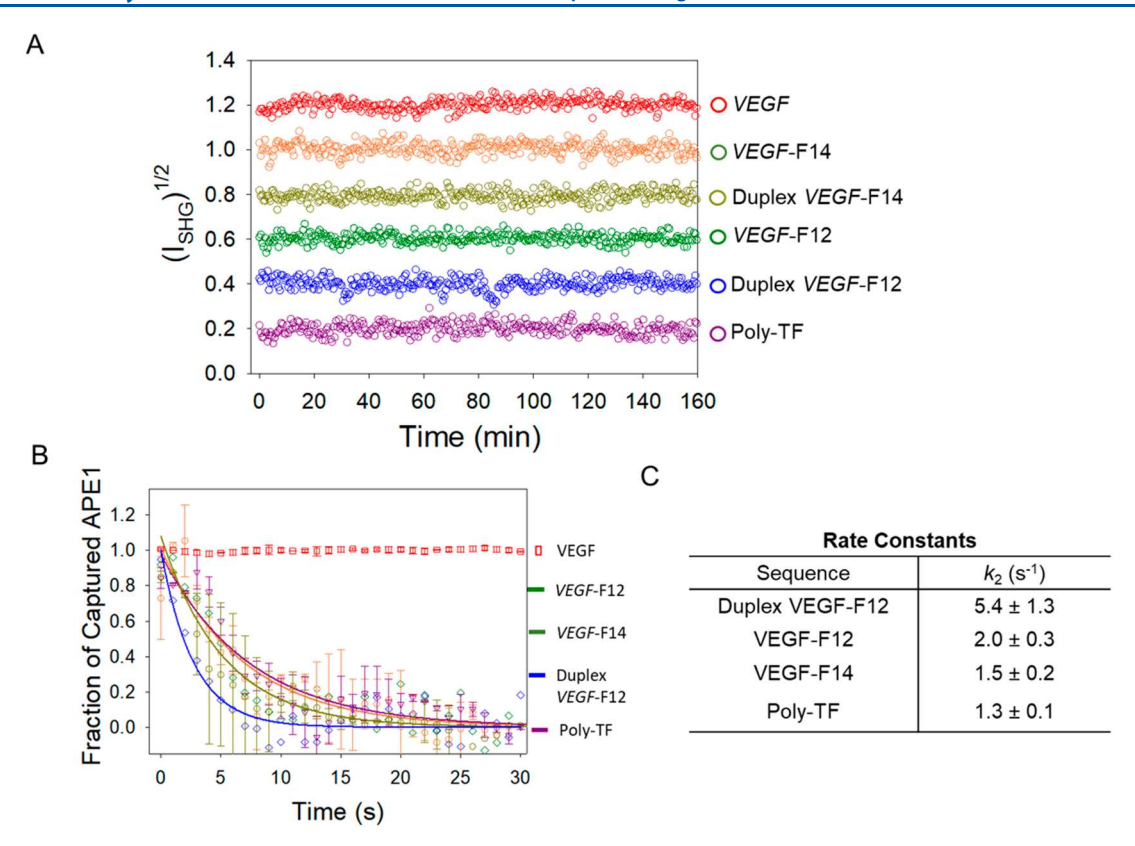


Figure 3. Monitoring desorption of APE1 from the DNA by SHG. (A) Binding longevity between APE1 and the DNA substrates was monitored by SHG for 160 min. (B) SHG desorption assay of bound APE1 upon injection of 2 mM Mg²⁺ into the analysis flow cell. (C) Table of desorption rate constants obtained from fitting the data in panel B.

removed before the binding studies. Therefore, a control binding study was conducted with the hexahistidine tag removed from APE1 to find that binding to the wild-type VEGF G4 was the same as that observed with the C-terminal tagged protein (Figure S3). To study whether the surface density of the G4 folds impacted the measured value, a 5-fold reduction in surface coverage of the G4 DNA was conducted by mixing the G-rich strand with a single-stranded poly-T₁₅ DNA in a 1:5 ratio. The results of the study found a similar binding profile and binding constant as measured at the higher density (Figure S4). This study also supports the conclusion that the SHG analysis monitored specific binding between APE1 and the G4 folds; if electrostatic nonspecific binding was occurring, the mixed G4 single-stranded DNA binding curve would not mirror that of the G4 alone. These studies support the conclusion that values obtained by SHG analysis result from a native domain of APE1 binding to a single G4 fold on the silica surface.

In the final set of experiments, the DNA-immobilized surfaces saturated with bound APE1 were rinsed with excess buffer to monitor the longevity of the interactions. Following the SHG signal out to 160 min identified no detectable desorption (Figure 3A). In the absence of Mg²⁺, the DNA-protein interactions can persist on time scales that are more than biologically feasible. The endonuclease APE1 utilizes Mg²⁺ as a cofactor for catalyzing phosphodiester bond hydrolysis 16 leading us to address how the presence of this divalent metal impacts the DNA-protein interactions. The DNA-surface bound proteins were then exposed to 2 mM Mg²⁺ in the flow cell, and the SHG signal was monitored (Figure 3B). These studies found exponential decay in the

SHG signal induced by the presence of Mg^{2+} , in which the curves were fit to identify rates for protein release (Figure 3B,C). The release of APE1 from the F-containing duplex DNA was $5.4 \pm 1.3 \text{ s}^{-1}$ and from the single-stranded poly-TF strand was $1.3 \pm 0.1 \text{ s}^{-1}$. The *VEGF* G4 with a loop F (position 12) released the bound APE1 in the presence of Mg^{2+} with a rate of $2.0 \pm 0.3 \text{ s}^{-1}$, while the *VEGF* G4 with a core F (position 14) was released with a rate of $1.5 \pm 0.2 \text{ s}^{-1}$. Interestingly, the native *VEGF* G4 without an F lesion continued to be bound by APE1 in the presence of Mg^{2+} for the duration of the analysis (30 s). These final experiments identify that when excess Mg^{2+} is present, disruption of the binary complex occurs resulting in the release of the protein from the surface into the solution.

The utilization of SHG enabled the demonstration that APE1 binds all three DNA structural contexts studied (singlestranded, double-stranded, and G4) with an F residue in an ordered and specific fashion. These results address the unanswered question from the fluorescence anisotropy experiments regarding whether the APE1 binding with the VEGF G4 substrates was specific or nonspecific: The binary complexes interact with specificity. APE1 binds single-stranded and double-stranded structures with K_d values >200 nM (Figure 2C), which is in the upper range of prior studies. Three possible reasons could account for the slightly weaker binding affinity observed herein: (a) the absence of Mg²⁺ in this analysis; (b) the orientation-specific signal observed by SHG only detects ordered binding, not convoluted by nonspecific interactions that contribute to positive signals in binding studies performed by other methods; and (c) specifically for the duplex DNA context, the high binding constant measured

could result from APE1 cleavage of the strand on the surface while the protein maintains binding to the nicked product strand. The high nM K_d value determined for the duplex is consistent with the product (i.e., nicked strand) binding being studied based on previous reports, 20 although the present data cannot rule out any of the three possibilities for the higher K_d value measured by SHG. Binding of APE1 to the nicked product in the single-stranded context is unlikely because cleavage of the strand would lead to release from the surface and loss of signal that was not observed before the addition of Mg^{2+} ; however, this cannot be ruled out with the present data.

In contrast, APE1 binds with orientation specificity to VEGF G4s bearing an AP modeled with an F with more than a 2-fold reduction in K_d value (~100 nM) compared to the canonical DNA strands. The K_d values found were lower for VEGF with a loop F at position 12 than an F in the core at position 14 (K_d values: 83 vs 134; Figure 2B); the greater disruption of the G4 fold with a core lesion, which is not observed with the loop lesion, suggests APE1 binds with greater affinity to the more stable G4 fold (Figure S2). This final observation is further supported by the greatest measured binding affinity occurring between APE1 and the native VEGF G4 without an F site. Our prior fluorescence anisotropy studies found the presence of Mg²⁺ led to the greatest APE1-G4 affinities, and the finding herein that the tight binding was maintained likely results from the residual Mg²⁺ bound by the recombinant APE1 used in the studies.⁴ The low nanomolar K_d value determined for APE1 binding the VEGF G4 structure is also consistent with a value found for the same protein binding the human telomere G4 fold.¹⁷ Importantly, it was discovered that APE1 binds the VEGF G4 folds with greater specificity, based on the present SHG measurements.

The release of DNA-bound APE1 by the addition of 2 mM Mg²⁺ to the running buffer produced desorption kinetics that were similar for each of the different DNA structures studied with F $(1.3-5.0 \text{ s}^{-1}; \text{ Figure 3B})$. The desorption of the protein could occur when excess Mg²⁺ is present resulting in APE1 releasing the cleaved VEGF G4 strands. Rapid release of the product by excess Mg²⁺ has been documented.²¹ Solution studies were conducted to monitor the cleavage yields catalyzed by APE1 for the F-containing VEGF G4 folds to find <5% cleavage occurred after 1 h of incubation (Figure S5); thus, APE1 cleavage of the G4 folds on the surface is not supported by these solution-phase experiments. The G4 folds are plastic structures known to change topologies in the presence of Mg²⁺, which was noted for these sequences in our prior work.⁴ Moreover, APE1 binding to Mg²⁺ is disordered, ²² and a change in the solution concentration may impact the pliable binding of the metal. A possibility for APE1 desorption from the VEGF G4s bearing an F site when Mg2+ was added may result from structural shifts in the DNA, protein, or both causing the release observed. Why this does not occur with the native VEGF G4 during the time of the analysis is not understood at present, although this G4 fold was not impacted by Mg²⁺ based on our prior CD studies,⁴ which may explain the unobserved change with the divalent metal addition. It is noteworthy that, in cellulo, Mg²⁺ concentrations can range from 1 to 20 mM depending on cell type; a small fraction of total Mg²⁺ is "free" and not already coordinated to other sites in the cell (e.g., (d)NTPs, RNA, Mg²⁺-binding proteins).^{23,24} Thus, in the cell, the APE1 release kinetics from bound DNA are likely much slower than measured in the present studies with 2 mM free Mg²⁺ added to the flow cell. Future analyses with

APE1 mutant proteins that are catalytically inactive in the presence of ${\rm Mg}^{2+}$ but binding competent are needed as well as mutants to address the role of the N-terminal disordered domain for binding promoter G4 folds.

CONCLUSIONS

Cellular oxidative stress results in changes to the mRNA profile.² One proposed pathway leading to these mRNA expression changes is the oxidation of a G base in a promoter potential G-quadruplex sequence to yield OG. The OG serves to localize the DNA repair process for removal of the damaged base yielding an intermediate AP that drives the remodeling of duplex DNA to a G4 fold with the assistance of APE1.4 Binding between APE1 and the G4 serves as a hub for transcription factor recruitment for gene regulation. Binding between APE1 and the VEGF G4 was previously studied by fluorescence anisotropy in solution; however, this experimental approach could not rule out nonspecific binding between the two biopolymers. Herein, an SHG assay was utilized because the method is label-free with high sensitivity and is insensitive to randomly ordered nonspecific adsorption that provides information beyond what can be obtained by fluorescence-based approaches.⁷ The SHG analysis found nanomolar dissociation constants between APE1 and VEGF G4 folds with AP at either loop or core positions in the DNA noncanonical structures (Figure 2D). The dissociation constants measured for APE1 binding the G4 folds in solution devoid of additional Mg2+ were lower in value than those found for APE1 binding duplex and single-stranded controls (Figure 2D). More importantly, the APE1–G4 interactions are specific because SHG signals were observed suggesting protein domains provide binding pockets for the G4 folds. Monitoring the APE1-G4 interactions by SHG identified the interaction occurs with specificity and is not a nonspecific charge-charge interaction that could not be ruled out by other solution-phase experiments. These studies provide a new example of the power of SHG to monitor biomolecule binding, in which the present partners were a DNA sequence capable of adopting different structures (i.e., duplex or G4) with the protein APE1. The work provides groundwork for future biochemical and biophysical experiments for interrogation of APE1 interaction with G4 DNA as well as for other studies regarding protein-DNA binding analyses.

ASSOCIATED CONTENT

Supporting Information

The Supporting Information is available free of charge at https://pubs.acs.org/doi/10.1021/acs.analchem.2c02951.

Complete experimental methods, circular dichroism analysis to verify *VEGF* G4 folding, SHG analysis of APE1 with the hexahistidine tag removed, SHG analysis of APE1 binding the *VEGF*-F12 G4 at a lower surface density of the DNA, and monitoring APE1 activity on the *VEGF* G4s with an F site by polyacrylamide gel electrophoresis (PDF)

AUTHOR INFORMATION

Corresponding Authors

John C. Conboy – Department of Chemistry, University of Utah, Salt Lake City, Utah 84112-0850, United States; orcid.org/0000-0003-0023-642X; Email: conboy@chem.utah.edu

Analytical Chemistry Article pubs.acs.org/ac

Cynthia J. Burrows – Department of Chemistry, University of Utah, Salt Lake City, Utah 84112-0850, United States; orcid.org/0000-0001-7253-8529; Email: burrows@ chem.utah.edu

Authors

Aaron M. Fleming - Department of Chemistry, University of Utah, Salt Lake City, Utah 84112-0850, United States; © orcid.org/0000-0002-2000-0310

Renee Tran - Department of Chemistry, University of Utah, Salt Lake City, Utah 84112-0850, United States

Carla A. Omaga – Department of Chemistry, University of Utah, Salt Lake City, Utah 84112-0850, United States; orcid.org/0000-0002-9189-6812

Shereen A. Howpay Manage - Department of Chemistry, University of Utah, Salt Lake City, Utah 84112-0850, United States

Complete contact information is available at: https://pubs.acs.org/10.1021/acs.analchem.2c02951

Notes

The authors declare no competing financial interest.

ACKNOWLEDGMENTS

This research was supported by the National Science Foundation (NSF 1953975) and a National Institutes of Health grant (R01 GM129267). The oligonucleotides were provided by the University of Utah Health Sciences Core facilities that are supported by the National Cancer Institute Cancer Support grant (P30 CA042014).

REFERENCES

- (1) Hudson, N. O.; Buck-Koehntop, B. A. Molecules (Basel, Switzerland) 2018, 23 (10), 2555.
- (2) Fleming, A. M.; Ding, Y.; Burrows, C. J. Proc. Natl. Acad. Sci. U.S.A. 2017, 114, 2604-2609.
- (3) Wang, R.; Hao, W.; Pan, L.; Boldogh, I.; Ba, X. Cell. Mol. Life Sci. **2018**, 75 (20), 3741–3750.
- (4) Fleming, A. M.; Howpay Manage, S. A.; Burrows, C. J. ACS Bio. & Med. Chem. Au 2021, 1 (1), 44-56.
- (5) Fleming, A. M.; Burrows, C. J. NAR Cancer 2021, 3 (3), zcab038.
- (6) Mergny, J. L.; Sen, D. Chem. Rev. 2019, 119, 6290-6325.
- (7) Tran, R. J.; Sly, K. L.; Conboy, J. C. Annu. Rev. Anal. Chem. 2017, 10 (1), 387-414.
- (8) Tran, R. J.; Lalonde, M. S.; Sly, K. L.; Conboy, J. C. J. Phys. Chem. B 2019, 123 (22), 4673-4687.
- (9) Kriech, M. A.; Conboy, J. C. J. Am. Chem. Soc. 2003, 125 (5), 1148-1149.
- (10) Nguyen, T. T.; Sly, K. L.; Conboy, J. C. Anal. Chem. 2012, 84 (1), 201-208.
- (11) Doughty, B.; Kazer, S. W.; Eisenthal, K. B. Proc. Natl. Acad. Sci. U. S. A. 2011, 108 (50), 19979-19984.
- (12) Sly, K. L.; Conboy, J. C. Anal. Chem. 2014, 86 (22), 11045-11054.
- (13) Schermerhorn, K. M.; Delaney, S. Biochemistry 2013, 52 (43),
- (14) Schuermann, D.; Scheidegger, S. P.; Weber, A. R.; Bjørås, M.; Leumann, C. J.; Schär, P. Nucleic Acids Res. 2016, 44 (5), 2187-2198. (15) Agrawal, P.; Hatzakis, E.; Guo, K.; Carver, M.; Yang, D. Nucleic Acids Res. 2013, 41 (22), 10584-10592.
- (16) McNeill, D. R.; Whitaker, A. M.; Stark, W. J.; Illuzzi, J. L.; McKinnon, P. J.; Freudenthal, B. D.; Wilson, D. M., 3rd Mutagenesis **2020**, 35 (1), 27–38.

- (17) Burra, S.; Marasco, D.; Malfatti, M. C.; Antoniali, G.; Virgilio, A.; Esposito, V.; Demple, B.; Galeone, A.; Tell, G. DNA Repair 2019, 73, 129-143.
- (18) Hoitsma, N. M.; Whitaker, A. M.; Beckwitt, E. C.; Jang, S.; Agarwal, P. K.; Van Houten, B.; Freudenthal, B. D. Nucleic Acids Res. **2020**, 48 (13), 7345–7355.
- (19) Maher, R. L.; Bloom, L. B. J. Biol. Chem. 2007, 282 (42), 30577-30585.
- (20) Izumi, T.; Schein, C. H.; Oezguen, N.; Feng, Y.; Braun, W. Biochemistry 2004, 43 (3), 684-689.
- (21) Masuda, Y.; Bennett, R. A.; Demple, B. J. Biol. Chem. 1998, 273 (46), 30360-30365.
- (22) Lipton, A. S.; Heck, R. W.; Primak, S.; McNeill, D. R.; Wilson, D. M., 3rd; Ellis, P. D. J. Am. Chem. Soc. 2008, 130 (29), 9332-9341.
- (23) Romani, A. Arch. Biochem. Biophys. 2007, 458 (1), 90-102.
- (24) Murphy, E. Circ. Res. 2000, 86 (3), 245-248.

□ Recommended by ACS

Distinctive Participation of Transcription-Coupled and Global Genome Nucleotide Excision Repair of Pyrimidine Dimers in the Transcribed Strand of Yeast rRNA Genes

Audrey Paillé, Antonio Conconi, et al.

JUNE 22, 2023 BIOCHEMISTRY

RFAD 🗹

Biophysical Characterization of Nucleolin Domains Crucial for Interaction with Telomeric and TERRA G-Quadruplexes

Yasmeen Khan, Mary K. Ekka, et al.

MARCH 23, 2023 BIOCHEMISTRY

READ **C**

G-Quadruplex Structures as a "Switch" Regulate ATF4 **Expression in Ferroptotic HepG2 Cells**

Miaomiao Liu, Jinku Bao, et al

FEBRUARY 01, 2023

ACS CHEMICAL BIOLOGY

READ C

Phase Separation Modulates the Formation and Stabilities of **DNA Guanine Quadruplex**

Zi Gao, Yinsheng Wang, et al.

MAY 24, 2023

JACS AU

READ 🗹

Get More Suggestions >